

# Frequency clustering of coupled phase oscillators on small-world networks

L.G. Morelli<sup>1,a</sup>, H.A. Cerdeira<sup>1</sup>, and D.H. Zanette<sup>2</sup>

<sup>1</sup> Abdus Salam International Center for Theoretical Physics, P.O. Box 586, 34100 Trieste, Italy

<sup>2</sup> Consejo Nacional de Investigaciones Científicas y Técnicas, Centro Atómico Bariloche and Instituto Balseiro, 8400 Bariloche, Argentina

Received 9 July 2004 / Received in final form 10 December 2004

Published online 25 February 2005 – © EDP Sciences, Società Italiana di Fisica, Springer-Verlag 2005

**Abstract.** We analyze the phenomenon of frequency clustering in a system of coupled phase oscillators. The oscillators, which in the absence of coupling have uniformly distributed natural frequencies, are coupled through a small-world network, built according to the Watts-Strogatz model. We study the time evolution and determine variations in the transient times depending on the disorder of the network and on the coupling strength. We investigate the effects of fluctuations in the average frequencies, and discuss the definition of the threshold for synchronization. We characterize the structure of clusters and the distribution of cluster sizes in the synchronization transition, and define suitable order parameters to describe the aggregation of the oscillators as the network disorder and the coupling strength change. The non-monotonic behavior observed in some order parameters is related to fluctuations in the mean frequencies.

**PACS.** 05.45.Xt Synchronization; coupled oscillators – 89.75.Hc Networks and genealogical trees – 05.45.-a Nonlinear dynamics and nonlinear dynamical systems – 89.75.-k Complex systems

## 1 Introduction

Many physical, chemical, and biological systems are suitably modeled as large populations of coupled nonlinear oscillators [1,2]. In these models, each element is represented by an oscillator whose individual dynamics is described by a differential equation. The interaction between elements is introduced by coupling the evolution of their degrees of freedom. In many cases of interest, the strength of the coupling is given by a single parameter  $\varepsilon$ , but the coupling pattern between elements may be quite different depending on the nature of the interactions. In the global coupling scheme, every element interacts with all the others with the same strength [2,3]. Global coupling arises whenever the interaction propagates over the whole system in very short times as compared to the time scale of the individual dynamics, and its range is larger than the system size. Josephson junctions [4] and certain catalytic chemical reactions [5] are typical examples. A local coupling scheme is suitable when the interaction range is short and the oscillators receive a significant input only from their nearest neighbors [6]. Random coupling has also been considered [7,8], where the pattern of interactions is

modeled by a random matrix. The most prominent manifestation of collective evolution in these models is synchronization. As the coupling strength grows, the oscillators start to form synchronized groups, where one or more degrees of freedom of the different oscillators have the same value and follow the same trajectory in phase space. Above some critical value of the coupling strength, a phase transition occurs and all the oscillators become synchronized. Much work has been devoted to the characterization and understanding of the different aspects of synchronization phenomena, for various dynamical systems and coupling schemes [9–11].

Meanwhile, it has been pointed out that the network of interactions in many complex systems displays features of both ordered and random graphs [12]. In ordered networks the clustering coefficient is large, meaning that the neighbors of a given node have a high probability of being in turn mutual neighbors. In random networks the average distance between two nodes is small as compared to the system size, and grows with the logarithm of the number of nodes. Watts and Strogatz have proposed a model that interpolates between ordered and random networks and displays these two features [12]. It has been shown that high clustering coefficients along with short average distances are common to a variety of biological, social, and technological networks. Also, it has been found that the characteristic topology of these networks may have important consequences on dynamical processes taking place on

---

<sup>a</sup> *Current address:* Max Planck Institute for the Physics of Complex Systems, Nöthnitzer Strasse 38, 01187 Dresden, Germany  
e-mail: morelli@mpipks-dresden.mpg.de

them [13–17]. Hence it is relevant to consider the effects of network disorder on synchronization processes.

The synchronization of coupled oscillators on Watts-Strogatz networks has been studied recently [18–20]. The Kuramoto order parameter, quantifying the degree of phase coherence in the population, has been measured for different degrees of disorder. It has been found that disorder enhances phase synchronization, with the critical coupling strength decreasing monotonically as the network disorder grows. In this paper, we investigate the effects of disorder on the clustering process that leads to synchronization of the time-averaged frequencies.

## 2 Coupled oscillators on a Watts-Strogatz network

The model consists of  $N$  phase oscillators whose natural frequencies  $\omega_i$  are distributed with probability density  $g(\omega)$ . The oscillators are coupled through a Watts-Strogatz small-world network [12], which is built in the following way. We begin with a regular linear array of  $N$  nodes, where each node is linked to its  $K$  nearest neighbors to the right and to the left. Periodic boundary conditions are assumed. Nodes are thus arranged in a ring with  $2K$  links per node. We select a node and, with probability  $p$ , the link with its nearest neighbor to the right is rewired to a randomly chosen node in the network. Self connections and repeated connections are avoided. Then, we move counterclockwise around the ring and repeat this procedure with each node, until one lap is completed. This process is then repeated with the second nearest neighbor to the right of each node, and successively up to the  $K$ th nearest neighbor.

On each node of this network we place a phase oscillator [2]. The state of the oscillator is described by its phase  $\varphi_i$ , whose individual dynamics in the absence of coupling is given by  $\dot{\varphi}_i = \omega_i$ . Oscillators are coupled to their neighbors in the underlying small-world network. The dynamics of the coupled system is governed by the equations

$$\dot{\varphi}_i = \omega_i + \frac{\varepsilon}{k_i} \sum_{j \in \mathcal{V}_i} \sin(\varphi_j - \varphi_i), \quad (1)$$

where  $\varepsilon$  is the coupling parameter,  $k_i$  is the number of neighbors of node  $i$ , and  $\mathcal{V}_i$  is the set of neighbors of node  $i$ . In the case of a regular network,  $p = 0$ , the system is a ring of locally coupled oscillators [6]. For  $p = 1$  all the links in the network are rewired, and the coupling between oscillators is completely disordered.

## 3 Average frequency clustering

In this paper we focus on the synchronization of coupled oscillators in frequency space. Specifically, we consider the time-averaged frequencies [6, 21–23]

$$\bar{\omega}_i \equiv \langle \dot{\varphi}_i \rangle_\tau = \frac{1}{\tau} \int_{\tau_0}^{\tau_0 + \tau} \dot{\varphi}_i dt, \quad (2)$$

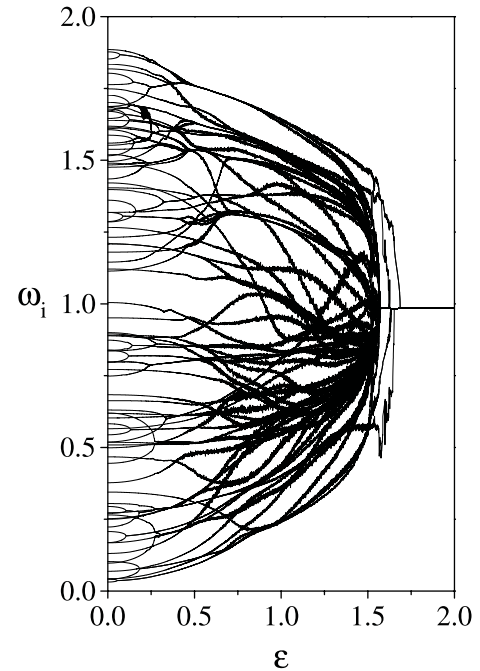


**Fig. 1.** Synchronization tree for an  $N = 100$  disordered network, with  $K = 3$  and  $p = 1$ . For this particular realization averages are done over  $\tau = 10^4$  time units. As coupling strength grows, the mean frequencies of different oscillators merge to form clusters. Fluctuations become more important as  $\varepsilon$  gets near its critical value.

where the time average is computed over an interval  $\tau$ , after transients of length  $\tau_0$  have elapsed. Both in globally and locally coupled systems, as the coupling parameter grows and synchronization progresses, some oscillators become entrained into clusters. Within each cluster, the average frequencies  $\bar{\omega}_i$  are identical. Our aim is to characterize the cluster structure during the synchronization transition, and analyze how this structure changes with the disorder of the interaction network.

Clustering is clearly visualized by means of a synchronization tree [21], where the average frequencies for all the oscillators is plotted as a function of the coupling strength  $\varepsilon$ . Figure 1 shows  $\bar{\omega}_i$  vs.  $\varepsilon$  in a system of  $N = 100$  oscillators, on a completely disordered network ( $p = 1$ ). A detailed examination of the synchronization tree reveals a rich variety of dynamical events. As we move from left to right, the collapse of two or more lines represents the formation of a cluster of synchronized oscillators. Occasionally, moreover, oscillators migrate between clusters, performing large jumps of average frequency.

We also see in Figure 1 that fluctuations in the average frequencies are very small at low coupling strengths and grow with  $\varepsilon$ , attaining their largest value just before the system synchronizes into a single cluster. To give a quantitative estimation of this fluctuations for different network architectures, we measure the time-averaged square deviation  $\langle (\langle \dot{\varphi}_i \rangle - \dot{\varphi}_i)^2 \rangle$  for all oscillators. Then, we average over the whole system and over different realizations of the small-world network with the same network disorder  $p$ , to

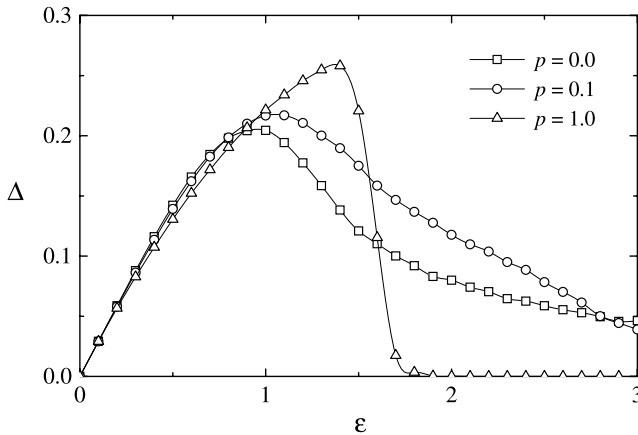


**Fig. 2.** Fluctuations around the mean values of the average frequencies. The curves correspond to different levels of disorder in the network connections, as indicated. Simulation parameters:  $N = 1000$  and  $K = 3$ . Averages over 100 realizations.

get  $\Delta$ , the mean value of fluctuations around the average frequencies. In Figure 2 we plot  $\Delta$  as a function of the coupling strength, for representative values of the network disorder  $p$ . Fluctuations grow from zero and then decrease as the system attains synchronization of the average frequencies. In disordered networks, fluctuations display a maximum and then fall quite abruptly. For  $p = 0.1$  and  $p = 0$  the decay of fluctuations is far more gradual. The value of  $\Delta$  gives an estimate of the instantaneous fluctuations of average frequencies. Moreover, the precision in the value of each frequency grows with the averaging time  $\tau$ . Therefore, average frequencies are determined with a resolution of order  $(\Delta/\tau)$ .

To attempt a statistical survey of the cluster structure as the coupling strength and the disorder parameter change, we must give a quantitative definition of clusters. We consider that two oscillators are synchronized—i.e. entrained in the same cluster—if their average frequencies  $\bar{\omega}_i$  differ by less than a certain threshold  $\delta_0$ . We define the cluster of element  $i$  as the set of elements  $j$  whose average frequencies satisfy

$$|\bar{\omega}_j - \bar{\omega}_i| \leq \delta_0, \quad (3)$$

and denote its size, given by the number of elements in this cluster, by  $\sigma_i$ . Note that even if  $j$  and  $j'$  are in the cluster of element  $i$ , it may happen that  $j'$  is not in the cluster of  $j$ . As we discuss below, the definition of this threshold is crucial in the observation of the cluster structure, as the relationship between fluctuations and this threshold can alter the observed patterns.

At a given value of the coupling parameter, the oscillators form clusters of different sizes. We denote by  $\rho(\sigma)$  the density of elements in clusters of a given size  $\sigma$ :

$$\rho(\sigma) = \frac{1}{N} \sum_{i=1}^N \delta(\sigma - \sigma_i). \quad (4)$$

Note that  $\rho(1)$  accounts for the fraction of elements that are not yet entrained in clusters. The distribution  $\rho(\sigma)$

gives detailed information on the cluster structure, and provides an accurate picture of the transition for different topologies of the network. A more concise quantitative description is obtained by defining suitable order parameters. Various ways to characterize the state of the system as far as the cluster structure is concerned [24,25], and to visualize the state of the system [6,21], have already been considered in the literature.

We now introduce the fraction  $s$  of elements whose cluster size  $\sigma_i$  is larger than one. This quantity accounts for the number of elements that are already entrained in clusters. This parameter is related in a simple way to the fraction of elements that have not yet entrained with any other element:  $s + \rho(1) = 1$ . For the uncoupled system we should have  $s = 0$ , as the oscillators do not form clusters. However, if the oscillators have close natural frequencies and the frequency space is crowded enough, some clusters may appear even in the absence of coupling, depending on the value of the threshold  $\delta_0$ . On the other hand, it is expected that for sufficiently strong coupling all the oscillators are in clusters of at least two elements, and  $s = 1$ . Still, this does not mean that complete synchronization has been attained.

An order parameter able to detect complete synchronization is the fraction  $d$  of pair distances  $|\bar{\omega}_j - \bar{\omega}_i|$ , measured in the space of average frequencies, which are smaller than  $\delta_0$ . An alternative order parameter is the ratio  $q$  of clusters with  $\sigma \geq 1$  to the total number of elements. This parameter equals the total number of particles (clusters plus non-entrained oscillators) over  $N$ . It differs from  $s$  because it includes isolated elements.

Finally, the number of clusters  $C$  with  $\sigma > 1$  gives yet another way to describe the state of the system during the transition. As the coupling strength is increased from zero, clusters start to form and the value of  $C$  grows. On the other hand, as complete synchronization is approached for large values of  $\varepsilon$ , the number of clusters must decrease to one. Thus, the plot of  $C$  vs.  $\varepsilon$  is expected to display a maximum for some value of the coupling strength.

## 4 Numerical results

We have performed extensive numerical simulations of the system in order to characterize the influence of disorder in the clustering process that leads to synchronization. The results presented in this section correspond to networks of  $N = 10^3$  oscillators and connectivity  $K = 3$ . In all cases, averages have been performed over more than  $10^2$  realizations. For each realization we generate a new small-world network, and new random values for the initial phases  $\varphi_i(0)$  and for the natural frequencies are chosen. Natural frequencies are uniformly distributed in the interval  $(\bar{\omega} - \delta\omega, \bar{\omega} + \delta\omega)$ , with  $\bar{\omega} = 1$  and  $\delta\omega = 1$ . Because of the rotational symmetry of the system, in fact, the value of  $\bar{\omega}$  can be fixed arbitrarily without generality loss. As for the frequency dispersion, it is known from the case of globally coupled oscillators that increasing  $\delta\omega$  results in a higher coupling strength at the synchronization

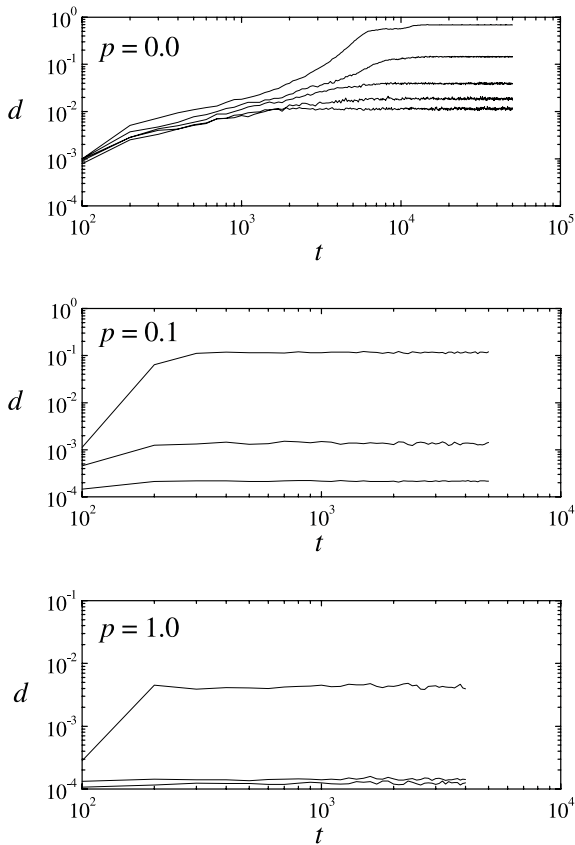


**Fig. 3.** Time dependence of order parameter  $d$ , on  $N = 1000$  networks, with  $K = 3$ . Time averages are computed every  $\tau = 100$  units of time. In the top panel  $p = 0$  and the curves correspond to  $\varepsilon = 4, 6, 9, 12$  and  $20$ , from bottom to top. In the central panel  $p = 0.1$  and the curves correspond to  $\varepsilon = 1, 2$ , and  $3$ . In the bottom panel  $p = 1$  and  $\varepsilon = 0.5, 1$ , and  $1.5$ .

transition [3]. The same behavior is found in our model, though we do not discuss such effect in detail.

We integrate numerically the equations of motion (1) using a fourth-order Runge-Kutta algorithm. The time step is  $\delta t = 0.1$  in most cases, and  $\delta t = 0.01$  when it is necessary to integrate for longer times, as for  $p = 0$ . The time unit is defined as  $\delta t^{-1}$  integration steps. We compute the instant value of the frequency of each oscillator as the right hand side of (1) at each time step, and calculate its average following equation (2).

In disordered networks, with  $p > 0$ , transients are relatively short. In Figure 3 we plot the time dependence of the parameter  $d$  for different network disorders and various coupling strengths. The time-dependent value of  $d$  has been calculated by averaging over 100 time steps. For  $p = 0.1$  and  $p = 1$  transients are always much shorter than  $10^3$  time units, regardless of the value of the coupling strength. On the other hand, for ordered networks,  $p = 0$ , much longer transients occur in the intermediate coupling regime, as seen in the top panel. Accordingly, we have waited for  $10^3$  time units before starting to record the frequencies on networks with  $p > 0$ , while we have used adaptive transient times on ordered networks.

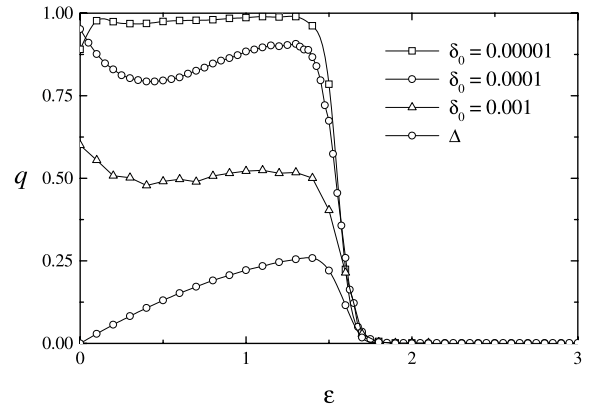


**Fig. 4.** Non-monotonic behaviour of  $q(\varepsilon)$ . The particular features of the clustering process depend on the value of the threshold  $\delta_0$ . Results obtained with  $N = 1000$ ,  $K = 3$ , and  $p = 1$ . Time averages done over  $\tau = 4000$  time units. We also plot  $\Delta$  for reference (bottom curve).

#### 4.1 Effects of frequency resolution and average times

It is beyond the scope of this paper to present an exhaustive study of the effects induced by the variation of the threshold  $\delta_0$ . Nevertheless, it has to be stressed that the value of  $\delta_0$  is of crucial importance for the description of the synchronization transition, as it defines the size of clusters. As we see below, it can alter significantly the observed cluster distribution. A large value of  $\delta_0$  results in the detection of spurious clusters even at very low coupling strengths. In fact, the natural frequencies lie closer to each other if we keep fixed the distribution  $g(\omega)$  and increase the number  $N$  of oscillators. As the value of  $\delta_0$  is decreased, a higher coupling strength is needed to bring the oscillators to such short distances in frequency space. In any case, the threshold should be larger than the resolution in the average frequencies which, as discussed above, is of order  $\Delta/\tau$ .

Figure 4 shows the behavior of the order parameter  $q$  as a function of the coupling strength  $\varepsilon$  for different values of the threshold  $\delta_0$ , in a disordered network. Time averages have been performed over  $\tau = 4000$  time steps. A sharp transition occurs at  $\varepsilon \approx 1.6$ , regardless of the threshold value. For the smallest value of the threshold,  $\delta_0 = 10^{-5}$ , the order parameter remains almost constant until the transition. But we see that as the value of the threshold is changed to  $\delta_0 = 10^{-4}$ , a non-monotonic behavior develops. This may seem striking at first sight, since it is expected that increasing the coupling strength should result in a reduction in the fraction of particles, as more and larger clusters are formed and more distances become smaller than  $\delta_0$ . Instead, we find that the value of  $q(\varepsilon)$  rises around  $\varepsilon \approx 1$ , before the system undergoes the synchronization transition and all distances fall below  $\delta_0$ . This non-monotonic behavior is related to the size of fluctuations in the average frequencies. Their growth makes some oscillators to leave their clusters, as the distances between pairs are no longer below the threshold. Finally, when the threshold is large enough ( $\delta_0 = 10^{-3}$  in the figure), a

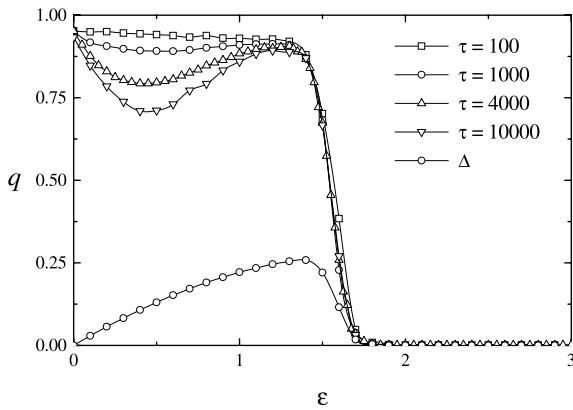


**Fig. 5.** Non-monotonic behaviour of  $q(\varepsilon)$  for different time spans  $\tau$ , as indicated. Here the value of the threshold is the same for all curves,  $\delta_0 = 10^{-4}$ , and simulation parameters are  $N = 1000$ ,  $K = 3$  and  $p = 1$ . When averages are done over short time spans, large fluctuations prevent the oscillators from forming clusters at low coupling strengths, until the transition point. For larger time spans, fluctuations are smaller at low coupling values and the system shows an early clustering process, with a non-monotonic behaviour as fluctuations overcome the precision of the time averages. Numerical results for the fluctuations  $\Delta$  are also shown (bottom curve).

wealth of spurious clusters exist even in the absence of coupling, simply because the natural frequencies are too crowded to be discriminated by the threshold.

A similar situation is found in Figure 5. Now the value of the threshold is kept constant at  $\delta_0 = 10^{-4}$ , and the time span  $\tau$  is varied. For short time spans, a monotonic decrease of the fraction of particles is observed, with a sharp transition around  $\varepsilon \approx 1.6$ . For larger values of  $\tau$ , however, fluctuations are reduced for low coupling strengths, and  $q$  decreases rapidly. But above some coupling strength the time span is no longer enough to reduce the large fluctuations occurring as the critical value of  $\varepsilon$  is approached. Consequently,  $q$  starts to grow again until the critical coupling is attained and the system synchronizes.

## 4.2 Clustering and synchronization

We have shown that the relationship between the time span  $\tau$  and the value of the threshold  $\delta_0$  plays a crucial role in defining the observed cluster structure and the particular features of the transition. In the following we fix  $\tau = 4000$  to compute the time averages  $\bar{\omega}_i$ , and  $\delta_0 = 10^{-4}$ , satisfying the relation  $\delta_0 > \Delta/\tau$ .

In Figure 6 we show the dependence of the order parameters  $s$  and  $d$  with the coupling strength  $\varepsilon$ . We first discuss the behavior of  $s$  for highly disordered networks,  $p = 0.4$  and  $p = 1$ . The fraction of elements in clusters grows with the coupling for small values of  $\varepsilon$ . Around  $\varepsilon = 0.5$ ,  $s$  attains a maximum and starts to decrease. At this point, the growing fluctuations have become strong enough to destabilize the already formed clusters, and the number of entrained oscillators falls. Looking back at Figure 2, we see that for  $p = 1$  fluctuations

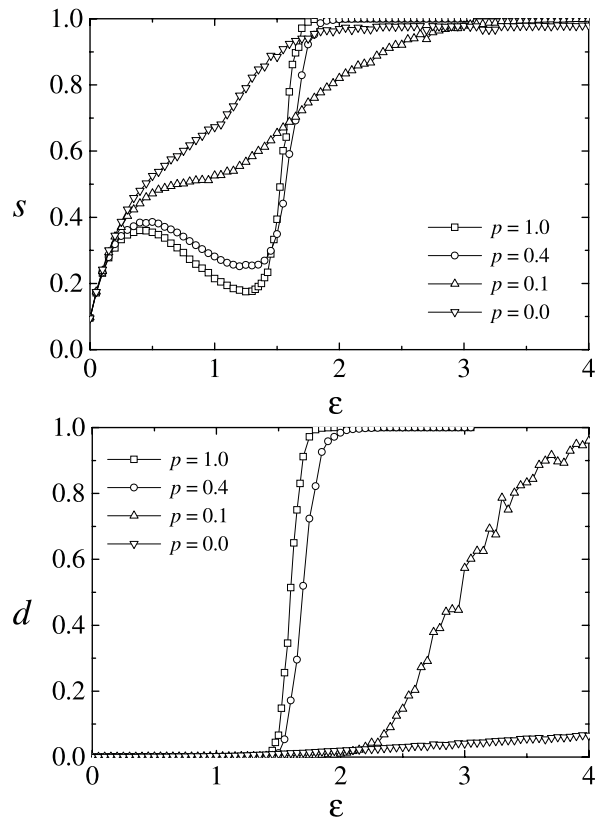


**Fig. 6.** Order parameters as a function of coupling strength for different networks. The plot of  $s$  vs.  $\varepsilon$  is shown in the top panel. In the bottom panel we plot  $d$  vs.  $\varepsilon$ . See discussion in the text. Simulation parameters:  $N = 1000$ ,  $K = 3$ ,  $\tau = 4000$  and  $\delta_0 = 10^{-4}$ .

grow with  $\varepsilon$  until a maximum is reached, and then decay abruptly. The coupling strength is then sufficient to overcome the fluctuations and bring the oscillators back together. The value of  $s$  grows to one as all the oscillators are entrained into clusters.

For regular networks, on the other hand, the value of  $s$  grows steadily in a monotonous way from zero to one. In this case, fluctuations are not enough to produce a non-monotonic behavior of the fraction of entrained oscillators. However, we do observe a bump, around  $\varepsilon = 1$ , where the largest fluctuations occur (see Fig. 2). Networks with  $p = 0.1$  behave qualitatively as regular networks, as far as the number of entrained elements is concerned.

The order parameter  $d$ , on the other hand, characterizes the transition to complete synchronization. For low coupling strengths,  $d$  remains close to zero, regardless of the topology of the network. For disordered networks a sharp transition is observed in a narrow range of the coupling strength. Above this transition we find  $d = 1$ , with all the elements in the same cluster, and all pair distances smaller than the threshold  $\delta_0$ . Here it is clear that large disorder favors synchronization, as it has been already pointed out [18].

The fraction of distances below the threshold increases far more slowly on more regular networks, as in the case



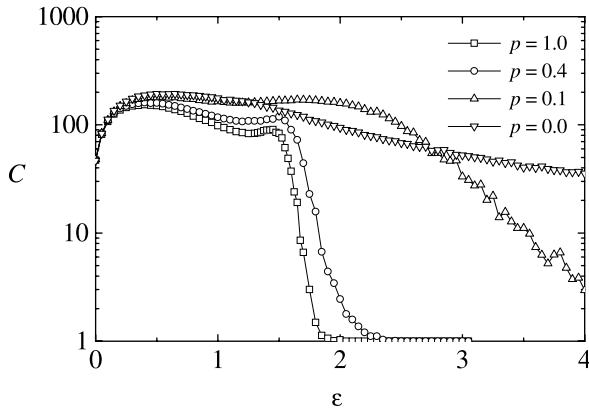


**Fig. 7.** The number of clusters  $C$  grows as coupling parameter is increased from zero, and after reaching a maximum value it decreases again to one, as complete synchronization is attained in the average frequencies. The fall of the number of clusters is shown to be steeper for more disordered networks. Simulation parameters as in Figure 6.

of  $p = 0.1$  and  $p = 0$ . In particular, in the case of  $p = 0$  this growth is very slow and it is not seen here for reasons of scale (see Fig. 9 below). We also find that the decay of fluctuations is slower for regular than for disordered networks (see Fig. 2). Turning back to the top panel of Figure 6, it is clear from the behavior of  $s$  that the clustering process starts at low values of the coupling. Now we see that these small clusters account for a very small fraction of the total number of pairs, resulting in a small value of  $d$ . It is remarkable that in the low coupling regime, the fraction of entrained elements grows faster for regular networks, but then fluctuations decay slowly and the fraction of entrained pairs grows slower for higher coupling strengths.

The total number of clusters during the synchronization process is shown in Figure 7 for the same realizations as in Figure 6. The value of  $C$  increases rapidly in the first stage of the process, as the oscillators gather together forming many small clusters. When nearly all the oscillators belong to a cluster ( $\sigma_i > 1$  for all  $i$ ), the number of clusters starts to decrease until only one cluster remains. We find that for disordered networks  $C$  remains at a large value until it drops abruptly at the synchronization transition. This behavior is less abrupt as the network becomes more ordered. On regular networks, the number of clusters remains high for a wide range of coupling strengths.

Comparing the plots of  $d$  and  $s$  gives additional insight on the clustering process. For regular networks the value of  $s$  grows rapidly while  $d$  remains small. This is an indication of many clusters being formed, but with a few elements in each one. The large value of  $s$  implies that almost all the elements are in clusters of at least two elements, while the small value of  $d$  means that a relatively small fraction of the pairs are at distances smaller than the threshold. For disordered networks, on the other hand, the clustering process seems to take place more abruptly, with the fraction of synchronized pairs growing fast, as soon as the condensation starts. Figure 8 shows the plot of  $d$  as a function of  $s$ . We see that in the intermediate range, when

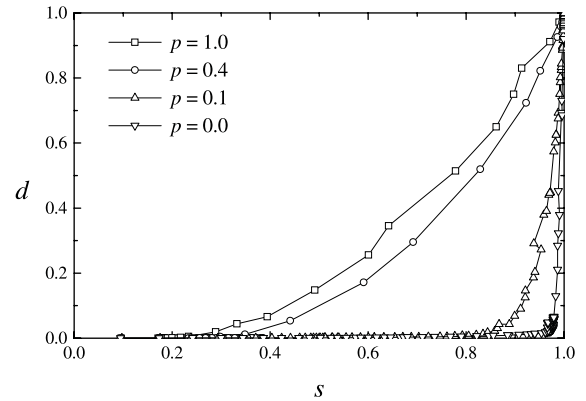


**Fig. 8.** Plot of  $d$  vs.  $s$  for different levels of network disorder. Disordered networks are closer to the identity function. In regular networks,  $s$  grows almost to one before  $d$  presents a significant change. The data plotted here is the same than in Figure 6.

the clustering process is developing, the values of  $d$  and  $s$  are closer in disordered networks. In regular networks, on the other hand,  $s$  grows almost to unity before  $d$  undergoes any significant change.

In Figure 6 we have shown the order parameters separately in order to compare results for different values of  $p$ . The plot range is limited to low coupling values, leaving the transition for  $p = 0$  networks out of view. Figure 9 shows the order parameters for  $p = 0, 0.1$ , and  $1$ , over a broader range of coupling strengths. In ordered networks clustering starts at very low coupling strength, and  $s$  grows fast as  $q$  decays until almost all the oscillators belong to some cluster. The value of  $d$  grows much slower, as stated above. For disordered networks, on the other hand, we find that all three order parameters have relatively sharp transitions. Nevertheless, there is a difference between  $s$  and  $d$ , as already discussed in the previous paragraphs.

So far, we have focused on the clustering process as the coupling strength changes, for different types of network architecture. Now we consider the dependence of the order parameters as a function of network disorder, when the coupling strength is kept constant. As can already be anticipated from Figure 6, some order parameters should present a non-monotonic behavior as a function of  $p$ . Such a non-monotonic dependence with the network disorder has already been observed in a variety of phenomena, including neural networks [16], biased diffusion [26], and even in networks of coupled oscillators [27]. In Figure 10 we show plots of  $q$  vs.  $p$  for selected values of the coupling strength, representative of different regimes. For weak coupling,  $\varepsilon = 1.5$ , the fraction of particles grows as the network disorder varies from  $p = 0$  to  $p \approx 0.4$ , and then presents a slight fall. The situation changes for higher coupling strength,  $\varepsilon = 1.75$  and  $\varepsilon = 2.0$ , where the non-monotonic behavior is more evident. The maximum of  $q(p)$  shifts to the left and becomes smaller as  $\varepsilon$  grows. Here we find again that the non-monotonic behavior is related to the fluctuations in the average frequencies. For

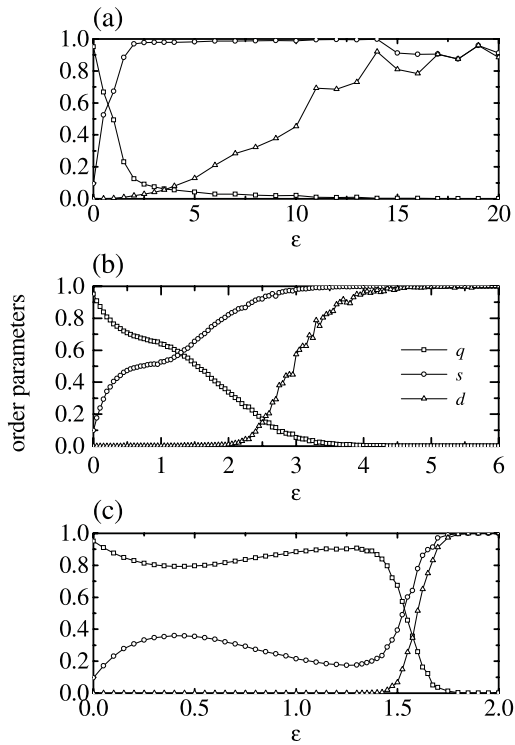


**Fig. 9.** Order parameters for different networks, with  $N = 1000$ ,  $K = 3$  and (a)  $p = 0$ , (b)  $p = 0.1$ , (c)  $p = 1$ . The whole transition range is presented here for  $p = 0$  and  $p = 0.1$ .

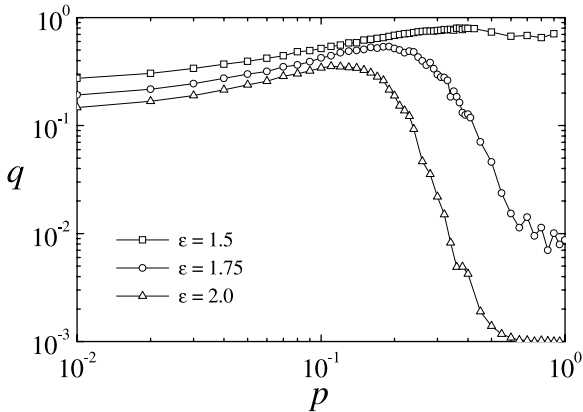


**Fig. 10.** Fraction of particles vs. network disorder for networks with  $N = 1000$ ,  $K = 3$ . The curves present a maximum at intermediate values of  $p$ . The non-monotonic behaviour is related to fluctuations in the average frequencies.

low coupling values, disordered networks display larger fluctuations. However, more disordered networks synchronize before, and thus  $q$  decays to zero when  $\epsilon$  is above the critical value.

Finally, we present some selected results for the distribution of cluster sizes (Fig. 11), in networks with  $p = 0$ , 0.1, and 1. For regular networks the cluster size distribution  $\rho(\sigma)$  has an exponential decay for low coupling values, and broadens for larger values of  $\epsilon$ , getting close to a uniform distribution around  $\epsilon = 6$ . This suggests that a

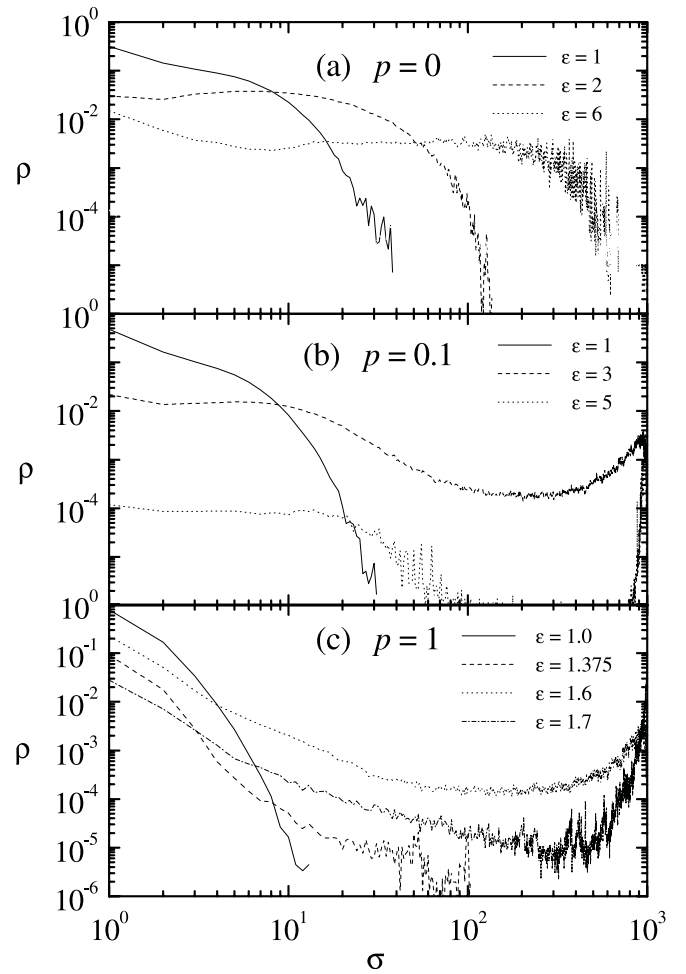


**Fig. 11.** Distribution of cluster sizes for different network architectures, and for some representative values of the coupling strength. In the top panel  $p = 0$ , in the center panel  $p = 0.1$ , and in the bottom panel  $p = 1$ . Parameters:  $N = 1000$ ,  $K = 3$ ,  $\tau = 4000$ ,  $\delta_0 = 10^{-4}$ , and averages over 1000 realizations.

mixture of many cluster sizes coexist in the intermediate range of coupling strength. As the coupling is increased from zero, clusters of all sizes are formed and merge subsequently. For  $p = 0.1$  the cluster distribution is similar at low coupling strengths, but for intermediate values of  $\epsilon$  it becomes bimodal, with a large number of small clusters and a maximum at high cluster sizes. For  $p = 1$ , the situation is even more evident. As coupling increases a minimum develops at intermediate cluster sizes. The distribution seems to fall as a power law for small cluster sizes and then has a maximum for large cluster sizes. This indicates that, as coupling grows from zero to its critical value, a large cluster is formed that captures the remaining oscillators and small clusters.

## 5 Summary and discussion

We have considered a network of coupled phase oscillators. The natural frequencies are drawn from a uniform

distribution, and the oscillators are coupled through a Watts-Strogatz small-world network. We studied the synchronization process in average frequency space. Defining adequate order parameters, we investigated the cluster structure as the disorder of the network  $p$  and the coupling strength  $\varepsilon$  change.

We have shown that the observed features of the clustering transition are sensible to the threshold  $\delta_0$  that defines the cluster size, and the time span  $\tau$  over which average frequencies are computed. We observed a non-monotonic behavior, both as a function of  $p$  and  $\varepsilon$ , and we found it to be related to the fluctuations in the average frequencies. In fact, when average frequencies are measured over a relatively short time span, fluctuations in their values prevent the oscillators from forming clusters. When averages are done over larger time spans, fluctuations are reduced and clusters are formed at low coupling values, but these clusters are destabilized as the coupling strength increases and fluctuations become larger (see Figs. 4 and 5).

We have studied extensively the synchronization transition for particular values of  $\tau$  and  $\delta_0$ . First we investigated the dependence of the order parameters with coupling strength, when network disorder is kept constant. We found, as previously reported [18], that disorder enhances synchronization. In regular networks, the fraction of oscillators in clusters grows quite rapidly, while the number of total pairs closer than the frequency threshold grows much more slowly. This indicates that many small clusters are formed at low coupling values, and gradually merge as the coupling strength is increased. The cluster size distribution shows that in the intermediate coupling range there are clusters of a variety of sizes, supporting this picture. For disordered networks the transition is sharper than for regular networks. Both the relationship between the order parameters  $s$  and  $d$ , and the cluster size distribution  $\rho(\sigma)$ , seem to indicate that, as the coupling strength is increased a large cluster is formed. This cluster grows as the remaining oscillators and smaller clusters merge with it. When the coupling strength is fixed, the dependence of the order parameters with network disorder  $p$  also shows an interesting non-monotonic behavior. This kind of behavior, which has been also found in other instances of dynamical systems, finds here its cause in the increasing of fluctuations.

A further study of the model we have presented should consider system size dependence. A careful determination of the critical values of  $\varepsilon$  and  $p$ , by means finite size scaling analysis, should allow us to build a detailed phase diagram. It would also be interesting to consider some extensions of the model. In particular, it should be of interest to contemplate link dynamics, where the interplay of oscillator dynamics and network linking could lead

to the emergence of network structure. This is clearly an important aspect for the study of dynamical systems with complex networks of interaction.

The authors wish to thank G. Abramson for fruitful discussions.

## References

1. A.T. Winfree, *The Geometry of Biological Time* (Springer, New York, 1980)
2. Y. Kuramoto, *Chemical Oscillations, Waves, and Turbulence* (Springer, Berlin, 1984)
3. S.H. Strogatz, *Physica D* **143**, 1 (2000)
4. D. Domínguez, H.A. Cerdeira, *Phys. Rev. Lett.* **71**, 3359 (1993)
5. N. Khrustova, G. Vesper, A. Mikhailov, R. Imbühl, *Phys. Rev. Lett.* **75**, 3564 (1995)
6. H. Sakaguchi, S. Shinomoto, Y. Kuramoto, *Prog. Theor. Phys.* **77**, 1005 (1987)
7. H. Daido, *Phys. Rev. Lett.* **68**, 1073 (1992)
8. J.C. Stiller, G. Radons, *Phys. Rev. E* **58**, 1789 (1998)
9. A.S. Pikovsky, M.G. Rosenblum, J. Kurths, *Synchronization: a universal concept in nonlinear sciences* (Cambridge University Press, 2001)
10. S.C. Manrubia, A.S. Mikhailov, D.H. Zanette, *Emergence of Dynamical Order: Synchronization Phenomena in Complex Systems* (World Scientific, Singapore, 2004)
11. S. Boccaletti, J. Kurths, G. Osipov, D.L. Valladares, C.S. Zhou, *Phys. Rep.* **366**, 1 (2002)
12. D.J. Watts, S.H. Strogatz, *Nature* **393**, 440 (1998)
13. M.E.J. Newman, D.J. Watts, *Phys. Rev. E* **60**, 7332 (1999)
14. M. Kuperman, G. Abramson, *Phys. Rev. Lett.* **86**, 2909 (2001)
15. D.H. Zanette, *Phys. Rev. E* **65**, 041908 (2002)
16. L.G. Morelli, G. Abramson, M.N. Kuperman, *Eur. Phys. J. B* **38**, 495 (2004)
17. L.G. Morelli, H.A. Cerdeira, *Phys. Rev. E* **69**, 051107 (2004)
18. H. Hong, M.Y. Choi, B.J. Kim, *Phys. Rev. E* **65**, 026139 (2002)
19. H. Hong, M.Y. Choi, B.J. Kim, *Phys. Rev. E* **65**, 047104 (2002)
20. M. Barahona, L.M. Pecora, *Phys. Rev. Lett.* **89**, 054101 (2002)
21. Z. Zheng, G. Hu, B. Hu, *Phys. Rev. Lett.* **81**, 5318 (1998)
22. El-Nashar et al., *Int. J. Bifurcat. Chaos* **12**, 2945 (2002)
23. El-Nashar et al., *Chaos* **13**, 1216 (2003)
24. D.H. Zanette, A.S. Mikhailov, *Phys. Rev. E* **57**, 276 (1998)
25. S.C. Manrubia, A.S. Mikhailov, *Phys. Rev. E* **60**, 1579 (1999)
26. D.H. Zanette, *Europhys. Lett.* **60**, 945 (2002)
27. Z. Hou, H. Xin, *Phys. Rev. E* **68**, 055103 (2003)